Quantitative correlations between wear behavior of $Ti_{1-x}Al_xN$ coating, structural transformations of the substrate WC-Co and coating itself during cathodic arc evaporation

Anna Kameneva*, *Natalia* Kameneva and *Vadim* Karmanov

Perm National Research Polytechnic University, Department of Innovative Technologies of Mechanical Engineering, 614990 Perm, Russia

Abstract. The temperature ranges of structural transformations in WC-Co and $Ti_{1-x}Al_xN$ in the process of cathode-arc evaporation are analyzed. The limiting values of the WC-Co temperature before the deposition of the coating correspond to 773 ... 873 K, after which the hardness of WC-Co and, as a consequence, the hardness of the composition WC-Co / $Ti_{1-x}Al_xN$ deteriorates. Analysis of the coating structural transformations made it possible to establish the structuring stages of the $Ti_{1-x}Al_xN$ coating during its deposition. Wear test was carried out for $Ti_{1-x}Al_xN$ coatings formed at each structuring stage. Wear test were carried out according to the finger-disk scheme at 300 K in coolant-cutting fluid on a laboratory friction machine. The wear behavior of the $Ti_{1-x}Al_xN$ coating are unstable at 773 K, then improve at 773 ... 853 K, stabilize with an increase in temperature to 963 K. The nanostructured $Ti_{1-x}Al_xN$ coating formed in the temperature range $T_{sub} / T_m = 0.18 ... 0.23$ have the best complex of wear properties in comparison with analogues.

1 Introduction

Despite many years of experience in the optimization and use of cathodic arc evaporation, reducing the instability of coating properties remains an urgent problem, in particular, in understanding the general patterns of formation of the real structure of the coating. Several scientific papers have discussed the relationship connection of coating wear behaviour with surface roughness [1, 2], surface contamination [3], surface temperature [4], and inclusions [5].

Structural stability and high wear behaviour up to 1273 K are mandatory protective requirements for coatings. Considering economic factors and competitive pressures, leading companies are particularly interested in extending the operating cycles of cutting tools and machine parts used in the automotive, aviation and space industries in the face of increasing thermo-mechanical loads applied to them [6].

* Corresponding author: annkam789@mail.ru

The article aim is to study the correlation between the wear properties of the $Ti_{1-x}Al_xN$ coating with the structural transformation of the substrate and the coating itself during its deposition by the CAE method. In addition, the critical temperatures of the materials of the substrate and $Ti_{1-x}Al_xN$ coatings will be established, above which coating properties deterioration occurs.

2 Material and methods

The $Ti_{1-x}Al_xN$ coatings, chosen as model ones, were formed by the cathodic arc evaporation (CAE) on automated unit URM3.279.048 equipped with two evaporators and four DC magnetron stutterers. Technological and temperature parameters of the deposition process are shown in Table 1.

Aluminum of technical purity EN AW-1085 was used as a material of low-melting cathode: Al-99.85 wt.%, Si-0.06 wt.%, Fe-0.08 wt.%, Cu-0.01 wt.%, Mn-0.02 wt.%, Mg-0.02 wt.%, Zn-0.02 wt.%, Ga-0.02 wt.%, Ti-0.008 wt.%, Others each 0.02 wt.%). The refractory cathode material was titanium of technical purity ERTi-1: Ti -99.42 wt.%, Si-0.08 wt.%, Fe-0.2 wt.%, C-0.05 wt.%, O-0.1 wt.%, N-0.04 wt.%, H-0.008 wt.%, Others each 0.1 wt.%.

Table 1. The formation processes parameters of the coating based on $Ti_{1-x}Al_xN$.

Cathode material	two cathodes	Ti
	one cathode	Al
The gas mixture pressure of argon and nitrogen, Pa		0.5, 0.6, 0.8, 1.0
The ratio of Ar/N_2 in the gas mixture, %		50:50
Arc current, A		75
Bias voltage, B		200, 280
Substrate temperature, equal to the initial coating temperature, $T_{sub}=T_{i.c.}$, K		673…1013 K or (0.15…0.23)T_m (T_m = 4350 K is the $Ti_{1-x}Al_xN$ coating melting temperature)
Cathode-substrate distance, mm		310±20
TiN sublayer deposition time, min		10
$Ti_{1-x}Al_xN$ coating deposition time, min		30
Test sample	material	hard alloy HG30
	size, mm	10x10x3

To change the substrate temperature, T_{sub}, and its heating rate, $V_{s.heat.}$, the high voltage value and the ionic cleaning duration of the substrate were raised. The $Ti_{1-x}Al_xN$ coating temperature, T_c, and its heating rate, $V_{c.heat.}$, were raised by increasing the gas mixture pressure P or the substrate bias voltage U_{bias} (Table 1).

The substrate surface temperature after its ion cleaning, as well as the temperature of a sublayer TiN and a $Ti_{1-x}Al_xN$ coating after their deposition was determined with the use of infrared non-contact pyrometer Thermix. The substrate rotation speed during the deposition of the $Ti_{1-x}Al_xN$ coating was 20 m / s.

The microstructure and defects of the $Ti_{1-x}Al_xN$ coatings were studied using an Ultra 55 field-emission electron microscope, depending on the substrate and coating temperature. The $Ti_{1-x}Al_xN$ coating microstructure at different stages of its structuring process was studied. EDX microanalysis system of microscope Ultra 55 we used to conduct a local X-ray microspectral analysis. Quantitative X-ray microanalysis was done by the MAR-3 unit at an accelerating voltage of 20 kV, probe current 20 nA, and the probe size5 μm [7-8].

Wear test were carried out according to the finger-disk scheme at 300 K in coolant-cutting fluid on a laboratory friction machine [9]. Finger - counterbody material was hard alloy HG30, disc material - stainless steel with $Ti_{1-x}Al_xN$ coatings. The fingers number was

3, and its sphere radius - R = 6.5 ± 0.25 mm. The axial loading on three fingers was Fa = 175 H, the linear sliding velocity of the finger - V = 0.68 m/s. The rubbing path of the fingers was L_r = 1500 m, the test duration - t = 740 s. The worn surfaces radius of coating was R = 7 mm. Profilograms of the worn $Ti_{1-x}Al_xN$ thin coating and finger surfaces were obtained and processed by a MarForm MMQ 400 high-precision roundness measurement device, running the MarShellMarWin software. The $Ti_{1-x}Al_xN$ coating friction coefficient (*f*), its wear rate by volume (I^v_{coat}) and by weight (I^m_{coat}), as well as, counterbody wear rate by volume (I^v_c) were determined.

3 Results and discussion

3.1 Structural transformations of the $Ti_{1-x}Al_xN$ coating during cathodic arc evaporation

In the structure formation of a $Ti_{1-x}Al_xN$ polycrystalline coating, the following stages proceed (Fig. 1):

1 - Globular stage, the formation and integration of globules (T_c=683...753 K, $V_{c.heat}$=1.9 K/min),

2 - Formation of {100} faces on globules (T_c=753...763 K, $V_{c.heat}$=2.2 K/min),

3- Nucleation and intergrowth of nuclei of the polycrystalline component of the $Ti_{1-x}Al_xN$ coating (T_c=763...773 K, $V_{c.heat}$=3.5 K/min),

4- Primary axial <100> texture formation, geometric selection (T_c=773...793 K, $V_{c.heat}$=4.0 K/min),

5* - The stage proceeds after the previously established stage 5 of geometric selection. The crystallites disorientation decreasing, their nanostructuring and the deposition of a continuous nanostructured $Ti_{1-x}Al_xN$ coating with a homogeneous fine structure in the forming direction (T_c=793…1013 K, $V_{c.heat}$=6.0 K/min),

5 - Formation of a primary polycrystalline $Ti_{1-x}Al_xN$ coating with a loose structure. The crystallites orientated relative to the substrate are divided by a network of parallel microvoids (T_c=793...963 K, $V_{c.heat}$=4.0 K/min),

6 - Texturing of crystallites in lamellar formations (T_c=963...1013 K, $V_{c.heat}$=4.0 K/min).

The stages rate of the $Ti_{1-x}Al_xN$ coating structuring depend on the thermal conditions of the substrate and the coating during its deposition: the substrate temperature with respect to the melting temperature of the T_{sub}/T_m coating and the coating heating rate $V_{c.heat}$, as well as the gas mixture pressure of nitrogen and argon *P* during coating deposition. The structural zone model of the $Ti_{1-x}Al_xN$ polycrystalline coating formed in the low-temperature region T_{sub}/T_m = 0.15-0.23 and *P* = 0.5-1.0 Pa is shown in Figure 1. A continuous nanostructured multilayer $Ti_{1-x}Al_xN$ coating with a preferred crystallographic orientation in the direction perpendicular to the substrate was formed at the stage 5* under optimal temperature conditions: $T_{sub} = T_{i.c.}$ = 793...1013 K = (0.182...0.23)·T_m and $V_{c.heat}$ = 6 K/min.

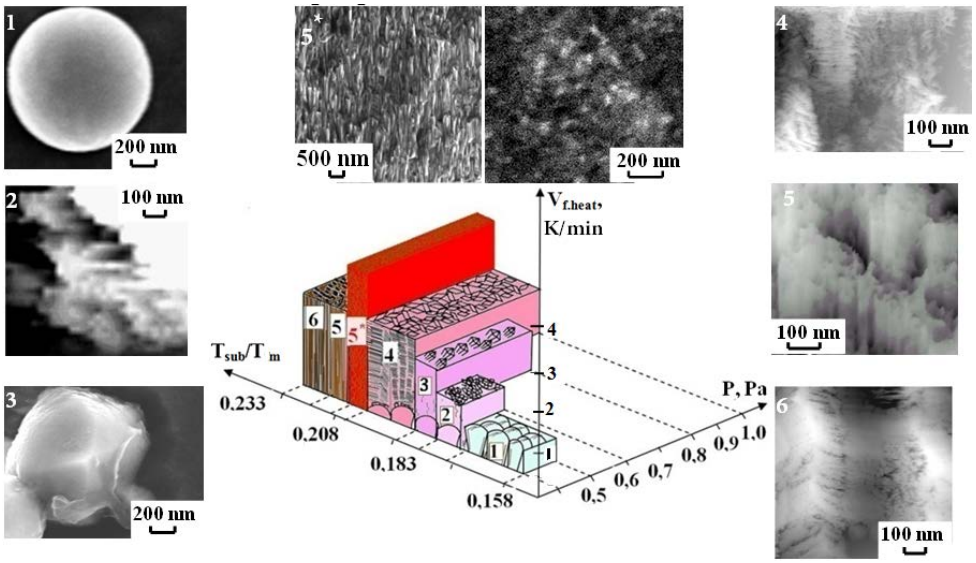

Fig. 1. Structuring stages of $Ti_{1-x}Al_xN$ coating and its structural zone model.

3.2 Structural transformations of the hard alloy HG30 during cathode-arc evaporation

The hot hardness of the HG30 alloy and of the HG30-$Ti_{1-x}Al_xN$ composition decreases from 4.49 μm up to 3.83 μm and from 21 GPa up to 19 GPa, respectively, if at T = 793 ... 963 K the plastic zone and the WC grain size increase to 6 μm (Fig. 2). At T = 963…1013 K the hot hardness continue to decline up to 3.06 GPa and 15 GPa, respectively (Fig. 2).

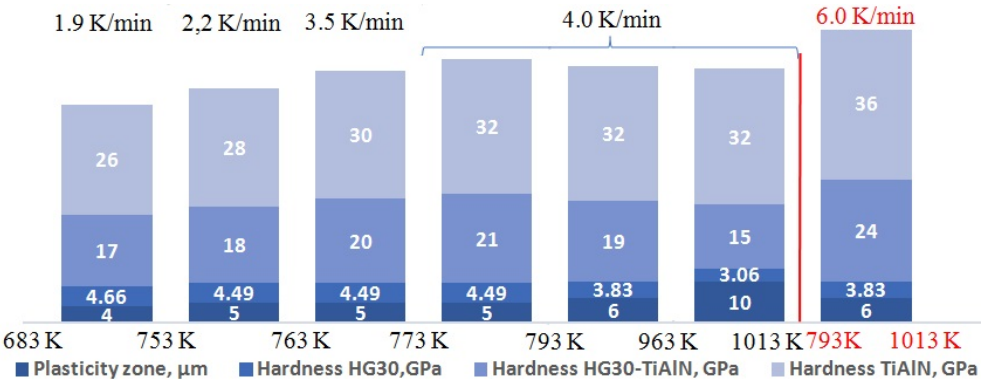

Fig. 2. Structuring stages of $Ti_{1-x}Al_xN$ coating and its structural zone model.

The thermal conductivity and thermal diffusivity of the hard alloy smoothly decrease with an increase in its temperature to 1073 K, and change insignificantly in the range of 1073 ... 1273 K [10]. The plasticity zone of all WC-Co grades from room temperature remains practically constant up to 773 K, and its size is similar to or slightly exceeds the WC-phase grain size. The values of the plastic zone up to T = 1073 K increase slightly, and at T> 1073 K they significantly exceed the average grain size WC [11]. This is the first reason in WC-Co hot hardness decrease.

The values of CTOD (crack tip opening displacement) and the plastic zone size of the WC-Co hard alloy remain almost constant up to 773 K, while at 973 K CTOD approaches

the value of plastic zone size. An abrupt increase in the average WC grain size results in unstable crack propagation and fatigue cracking of WC grains. A potential explanation for this is the change in the crack trajectory in the WC-Co microstructure caused by an increase in the plastically deformed volume around the crack tip at elevated temperatures [11]. This is the second reason in hot hardness decrease of WC-Co alloy and its defectiveness increase.

The reasons in WC-Co alloy hardness decrease is a change of hot hardness of the WC phase [12] and the Co phase [1] or boundary strength decrease of WC grains [10]. The WC-Co hardness leads to decline of HG30-$Ti_{1-x}Al_xN$ composition hardness (Fig. 2).

The limiting heating temperature for the hard alloy WC-Co before the $Ti_{1-x}Al_xN$ coatings deposition is 773…873 K and the optimum temperature for the beginning of coating structure formation corresponds to $T_{sub} / T_m = 0.2$. In the substrate heating process, stresses at the interface between $Ti_{1-x}Al_xN$ coating and substrate will be minimized, which could prevent the cracks formation and coating properties deterioration.

3.3 Quantitative correlations between wear behavior of $Ti_{1-x}Al_xN$ coating and its thermal state during cathodic arc evaporation

Quantitative correlations between wear behavior of $Ti_{1-x}Al_xN$ coating and its thermal state during cathode-arc evaporation are shown on Fig. 3.

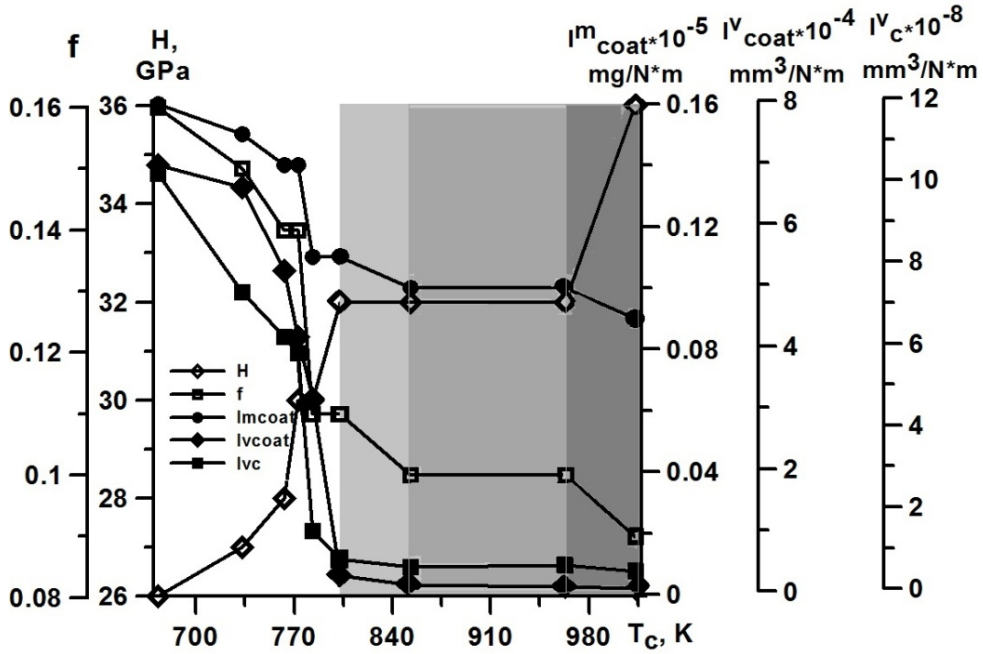

Fig. 3. Dependence of the tribological properties of $Ti_{1-x}Al_xN$ coatings on their temperature during deposition process.

Achievement of the coating hardness of 32 GPa in the range 773 ... 853 K is accompanied by a significant decrease in the coating friction coefficient, decline wear rate intensity by volume and by weight of the coating and the counterbody. The improvement in properties in a greater degree is caused not by the structural state of polycrystalline $Ti_{1-x}Al_xN$ coating, but by the optimal thermal state of the hard alloy. With a further increase in temperature to 963 K, the tribological properties of primary polycrystalline $Ti_{1-x}Al_xN$

coating with a loose structure do not change. A continuous nanostructured $Ti_{1-x}Al_xN$ coating with a homogeneous fine structure in the forming direction formed in optimal thermal interval 793...1013 K for it has the maximum hardness 36 GPa, minimum friction coefficient and minimum wear rate intensity of the coating and counterbody (table 2). The wear test results were compared with the tribological properties of similar $Ti_{1-x}Al_xN$ coatings deposited by different methods (Table 2).

Table 2. Tribological properties of $Ti_{1-x}Al_xN$ coatings.
V is the average volumetric wear of the film during the test, Δt/Δm is the wear resistance, h is the height of the worn segment, MS – magnetron sputerring.

Material coating	Deposition method	f	$\Delta t/\Delta m$, s/mg	$V\cdot10^{-3}$	$I_{coat}{}^{V}$ $\cdot10^{-4}$, $mm^3/N\cdot m$	$I_{coat}{}^{m}$ $\cdot10^{-5}$, $mg/N\cdot m$	$I_c{}^{V}$ $\cdot10^{-4}$, $mm^3/N\cdot m$	h, mm	Source
Ti-Al-N	CAE	0.5	–	–	–			–	[13]
Ti-Al-N	CAE	0.064…0.13	–	1.4…3.0 (mm^3)	–			–	[14]
Ti-Al-N	MS		510±40	–	–			–	[15]
Ti-Al-N	PVD	0.3…0.4	–	–	–			–	[16]
Ti-Al-N	CAE	0.5…0.6	–	–	–			–	[17]
Ti-Al-N/VN	MS	0.18…0.55	–	–	126*			–	[18]
Ti-Al-N	DC MS	0.88…1.5	–	–	–			–	[19]
Ti-Al-N	MS	0.5…1.1	–	–	–			–	[20]
Ti-Al-N	MS	0.88	–	–	–			–	[21]
Ti-Al-N	CAE	0.05…0.25	–	–	–			–	[22]
Ti-Al-N	PVD	1.0…1.2	–	–	–			–	[23]
Ti-Al-N	CAE	0.3	–	–	–			–	[24]
Ti-Al-N	CAE	0.05	–	3.0 (г)	–			–	[25]
Ti-Al-N	Pulse reactive MS	0.88	–	–	–			–	[21]
Ti-Al-N	CAE	>0.9	–	–	–			0.7	[22]
$Ti_{1-x}Al_xN$	CAE	0.09	740/ $5.6\cdot10^{-3}$	0.9 (mm^3)	0.05**	0.03**	0.43**	1.2 $\cdot10^{-2}$	

*Environment - humid air. **Environment - coolant-cutting fluid.

4 Conclusion

The influence of the temperature evolution of the hard alloy WC-Co and $Ti_{1-x}Al_xN$ coating on their physico-mechanical and thermo-physical properties is analyzed. The limiting heating temperature of the hard alloy WC-Co prior to the coating deposition beginning, as well as the coating temperature and its heating rate during deposition process have been established.

The coating structuring stages depending on its temperature are revealed. The formation temperature range of a nanostructured coating with a fine-grained surface structure has been determined.

Wear test of the coatings $Ti_{1-x}Al_xN$ formed at various structuring stages have been carried out. The first improvement in the tribological properties of the $Ti_{1-x}Al_xN$ coating is observed if heating temperature the WC-Co hard alloy before the $Ti_{1-x}Al_xN$ coatings deposition is lower than its limiting value 773…873 K.

The complex of maximum hardness, minimum friction coefficient, wear rate intensity of coating and hard alloy corresponds to a nanostructured $Ti_{1-x}Al_xN$ coating formed in the

optimal temperature conditions: T_{sub} = (0.182...0.23)·T_m (T_m=4350 K is the $Ti_{1-x}Al_xN$ melting temperature) and $V_{c.heat}$ = 6 K/min.

The results were obtained within the framework of the State task of the Ministry of Science and Higher Education of the Russian Federation (project no FSNM-2020-0026).

References

1. A. Anders, Cathodic Arcs: From Fractal Spots to Energetic Condensation (Springer Inc., New York, 2008).
2. B.A. Eizner, G.V. Markov, A.A. Minevich, *Deposition stages and applications of CAE multicomponent coatings*, Surface and Coatings Technology, v. **79(1-3)**, pp. 178-191 (1996).
3. Jüttner, I. Kleberg, *The retrograde motion of arc cathode spots in vacuum*, J Phys D: Appl Phys, v. **33,** pp. 2025–2036 (2000).
4. V.F. Puchkarev, A.M. Murzakayev, *Current density and the cathode spot lifetime in a vacuum arc at threshold currents*, J Phys D: Appl. Phys, v. 23, pp. 26–35 (1990).
5. A.A. Lisenkov, V.T. Barchenko, V.D. Goncharov, A.S. Zheukhin, *Vacuum-arc discharge on integral-cool cathode*, Instrument and Technologies, v. **34**, pp. 43-56 (2010).
6. C.M. Koller, S.A. Glatz, S. Kolozsvari, H. Bolvardi, P.H. Mayrhofer, *Thermal stability and oxidation resistance of architecturally designed Ti – Al – N- and Ti – Al – Ta – N-based multilayers*, Surface & Coatings Technology, v. **385**, 125444 (2020).
7. A.L. Kameneva, N.I. Cushentsov, E.M. Trofimov, *Studying the influence of technological and thermal conditions of Ti-Al-N films formation, using electro arc evaporation method, upon their structure, properties, formation mechanism and stages,* News of Per'm State Technical University Russia, v. **12(1),** pp. 63-75 (2010).
8. A.L. Kameneva, L.N. Guselnikova, T.O. Soshina, *An influence of a substrate voltage bias and temperature conditions on structure and phase modification in single-component ion-plasmas' films,* e-Journal of Surface Science and Nanotechnology, v. **9**, pp. 34-39 (2011).
9. A.L. Kameneva, *The influence of aluminum on the texture, microstructure, physical, mechanical and tribological properties of $Ti_{1-x}Al_xN$ thin films*, Res J Pharm Biol Chem Sci, v. **5(6)**, pp. 965-975 (2014).
10. A. Vornberger, J. Potschke, T. Gestrich, M. Herrmann, A. Michaelis, *Influence of microstructure on hardness and thermal conductivity of hardmetals*, International Journal of Refractory Metals & Hard Materials, v. **88**, 105170 (2020).
11. T. Teppernegg, T. Klünsner, C. Kremsner, C. Tritremmel, C. Czettl, S. Puchegger, S. Marsoner, R. Pippan, R. Ebner, *High temperature mechanical properties of WC-Co hard metals*, Int. Journal of Refractory Metals and Hard Materials, v. **56**, pp. 139–144 (2016).
12. A. Mubarak, E. Hamzah, M.R.M. Toff, *Study of macrodroplet and growth mechanisms with and without ion etchings on the properties of TiN coatings deposited on HSS using cathodic arc physical vapour deposition technique*, Materials Science and Engineering: A, v. **474(1-2)**, pp. 236-242 (2008).
13. D. Loktev, E. Yamashkin, *Basic types of wear-resistant coatings*, Nanoindustriya, v. **5**, pp. 24–30 (2007).
14. V.M. Beresnev, *Influence of multicomponent and multilayer coatings on the processes of friction and wear*, v. **2(4)**, FIP, pp. 214–219 (2004).

15. V.A. Buravikhin, V.P. Popov, V.I. Gorokhov, *On the reasons for the change in the temperature of the films in the process of their condensation in vacuum*, Physical and chemical processing of materials, v. **29(6)**, pp. 1314–1316 (1970).
16. Applied tool coating technology // www.star-su.com.
17. PLATIT// http://www.technopolice.ru/index.php/platit.html
18. P.H. Mayrhofer, C. Mitterer, L. Hultman, H. Clemens, *Microstructural design of hard coatings*, Progress in Materials Science, v. **51**. pp. 1032–1114 (2006).
19. K. Kutschej, P.H. Mayrhofer, M. Kathrein, P. Polcik, R. Tessadri, C. Mitterer, *Structure, mechanical and tribological properties of sputtered ti1-xalxn coatings with 0.5≤x≤0.75*, Surface and Coatings Technology, v. 200(7), pp. 2358–2365 (2005).
20. K. Chu, P.W. Shum, Y.G. Shen, *Substrate bias effects on mechanical and tribological properties of substitutional solid solution (Ti, Al)N films prepared by reactive magnetron sputtering*, Materials Science and Engineering: B. v. 131(1–3), pp. 62–71 (2006).
21. M.-K. Wu, J.-W. Lee, Y.-C. Chan, H.-W. Chen, J.-G. Duh, *Influence of bilayer period and thickness ratio on the mechanical and tribological properties of CrSiN/TiAlN multilayer coatings*, Surface and Coatings Technology, v. **206(7)**, 1886–1892 (2011).
22. R.-X. Huang, Z.-B. Qib, P. Sun, Z.-C. Wang, C.-H. Wu, Influence of substrate roughness on structure and mechanical property of TiAlN coating fabricated by cathodic arc evaporation, Physics Procedia, **v. 160–167**, pp. 1875–1892 (2011).
23. S. PalDey, S.C. Deevi, *Single layer and multilayer wear resistant coatings of (Ti,Al)N: a review*, Materials Science and Engineering, v. **A342**, pp. 58–792 (2003).
24. A.I. Ryabchikov, I.A. Ryabchikov, I.B. Stepanov, D.O. Sivin, S.E. Eremin, *Plasma Immersion Ion Charge State and Mass Spectrometer*, Proceedings of universities. Physics. v. **8**. pp. 530–533 (2006).
25. V.M. Beresnev, A.I. Fedorenko, V.I. Gritsenko, D.L. Perlov, *Investigation of the friction properties of composite coatings obtained by the vacuum arc method*, FIP, v. **1(2)**, pp. 180-183 (2003).